

REPORT DOCUMENTATION PAGE			Form Approved OMB NO. 0704-0188		
<p>The public reporting burden for this collection of information is estimated to average 1 hour per response, including the time for reviewing instructions, searching existing data sources, gathering and maintaining the data needed, and completing and reviewing the collection of information. Send comments regarding this burden estimate or any other aspect of this collection of information, including suggestions for reducing this burden, to Washington Headquarters Services, Directorate for Information Operations and Reports, 1215 Jefferson Davis Highway, Suite 1204, Arlington VA, 22202-4302. Respondents should be aware that notwithstanding any other provision of law, no person shall be subject to any penalty for failing to comply with a collection of information if it does not display a currently valid OMB control number.</p> <p>PLEASE DO NOT RETURN YOUR FORM TO THE ABOVE ADDRESS.</p>					
1. REPORT DATE (DD-MM-YYYY) 31-07-2018		2. REPORT TYPE Final Report		3. DATES COVERED (From - To) 1-May-2015 - 30-Apr-2018	
4. TITLE AND SUBTITLE Final Report: Toward the Computational Design of Iron-Based Chromophores			5a. CONTRACT NUMBER W911NF-15-1-0124		
			5b. GRANT NUMBER		
			5c. PROGRAM ELEMENT NUMBER 611102		
6. AUTHORS			5d. PROJECT NUMBER		
			5e. TASK NUMBER		
			5f. WORK UNIT NUMBER		
7. PERFORMING ORGANIZATION NAMES AND ADDRESSES North Carolina State University 2701 Sullivan Drive Admin Srvcs III, Box 7514 Raleigh, NC 27695 -7514			8. PERFORMING ORGANIZATION REPORT NUMBER		
9. SPONSORING/MONITORING AGENCY NAME(S) AND ADDRESS (ES) U.S. Army Research Office P.O. Box 12211 Research Triangle Park, NC 27709-2211			10. SPONSOR/MONITOR'S ACRONYM(S) ARO		
			11. SPONSOR/MONITOR'S REPORT NUMBER(S) 63854-CH.10		
12. DISTRIBUTION AVAILABILITY STATEMENT Approved for public release; distribution is unlimited.					
13. SUPPLEMENTARY NOTES The views, opinions and/or findings contained in this report are those of the author(s) and should not be construed as an official Department of the Army position, policy or decision, unless so designated by other documentation.					
14. ABSTRACT					
15. SUBJECT TERMS					
16. SECURITY CLASSIFICATION OF:			17. LIMITATION OF ABSTRACT UU	15. NUMBER OF PAGES	19a. NAME OF RESPONSIBLE PERSON Elena Jakubikova
a. REPORT UU	b. ABSTRACT UU	c. THIS PAGE UU			19b. TELEPHONE NUMBER 919-515-1808

RPPR Final Report

as of 21-Sep-2018

Agency Code:

Proposal Number: 63854CH

Agreement Number: W911NF-15-1-0124

INVESTIGATOR(S):

Name: Elena Jakubikova
Email: ejakubi@ncsu.edu
Phone Number: 9195151808
Principal: Y

Organization: **North Carolina State University**

Address: 2701 Sullivan Drive, Raleigh, NC 276957514

Country: USA

DUNS Number: 042092122

EIN: 566000756

Report Date: 31-Jul-2018

Date Received: 31-Jul-2018

Final Report for Period Beginning 01-May-2015 and Ending 30-Apr-2018

Title: Toward the Computational Design of Iron-Based Chromophores

Begin Performance Period: 01-May-2015

End Performance Period: 30-Apr-2018

Report Term: 0-Other

Submitted By: Elena Jakubikova

Email: ejakubi@ncsu.edu

Phone: (919) 515-1808

Distribution Statement: 1-Approved for public release; distribution is unlimited.

STEM Degrees: 5

STEM Participants: 7

Major Goals: This proposal focuses on computational studies of Fe(II)-polypyridine compounds as sensitizers in dye-sensitized solar cells (DSSCs). Starting from the prototype Fe(II)-polypyridine complexes ($[\text{Fe}(\text{bpy})_3]^{2+}$, $[\text{Fe}(\text{tpy})_2]^{2+}$, and $[\text{Fe}(\text{bpy})_2(\text{CN})_2]_0$), we aim to explore how various modifications to the bipyridine and terpyridine ligands, as well as their replacement by ligands of varying ligand field strength, impact the ground and excited state properties of these compounds relevant to the light-harvesting. Our aim is to identify the modifications that will result in the most favorable visible light absorption profiles and the most efficient interfacial electron transfer between the dye and the semiconductor in the DSSCs. In addition to computational investigation of Fe(II) chromophores, this proposal also seeks to develop computational approaches to reliable modeling of spin-state energetics in first-row transition metal complexes and interfacial electron transfer in dye-semiconductor assemblies.

There are 3 specific aims of this proposal: (1) increase the lifetime of metal-to-ligand charge transfer (MLCT) states of the Fe(II)-polypyridine complexes, (2) optimize absorption properties of Fe(II)-polypyridine compounds, and (3) speed-up the rate of the interfacial electron transfer (IET) between the excited chromophore and semiconductor.

Accomplishments: See the attached pdf document.

RPPR Final Report as of 21-Sep-2018

Training Opportunities: During the period of May 01, 2015 ending April 30, 2018, two postdoctoral researcher, 5 graduate students, 2 undergraduate students, and 1 high school student participated in this project's research activities. All the participants were trained in the basics of computational chemistry as applied to the study of inorganic compounds and photochemistry as well as the basics of electronic structure theory, with a special focus on the density functional theory. Graduate students also obtained training in the methods of molecular and quantum dynamics. All students acquired basic understanding of the coordination chemistry of iron complexes, and various photochemical processes that occur in the dye-sensitized solar cell. All trainees participated in the weekly group meetings of the Jakubikova group, as well as in weekly one-on-one meetings that give them the opportunity to discuss and present their work, and receive guidance from the PI.

Two graduate students obtained their PhD degree working on this project (David Bowman in 2015 and Sriparna Mukherjee 2017), both obtained postdoctoral positions upon graduation. One graduate student (Jessica Gonzalez-Delgado) obtained her MS degree in 2017, and is currently a PhD graduate student in Chemistry at NCSU. Two undergraduate student participants obtained undergraduate degrees, one in Chemistry and another one in Material Science Engineering. One of these students (Alexey Bondarev) is currently a graduate student in the Physics Department at Duke University.

The grant also provided a summer training opportunity for one high school student (David Torres) through the AEOP High School Apprenticeship Program, and one undergraduate student (Jason Brannock) through Undergraduate Apprenticeship Program. David Torres is currently an undergraduate student at NCSU, majoring in aerospace engineering.

Most of the trainees took part in various scientific meetings, presenting the results of their work in form of the poster and oral presentations (see results dissemination).

RPPR Final Report as of 21-Sep-2018

Results Dissemination: The work accomplished was disseminated in the form of (1) publications in the scientific journals, (2) thesis and dissertations, (3) oral and poster presentations at conferences, (4) during the seminar visits to other academic institutions and national laboratories, and (5) by outreach to local high schools. Overall, the Jakubikova group members have published 6 peer-reviewed journal articles, given 11 invited presentations at Universities and National Laboratories, 9 invited oral presentations as well as 18 poster and oral presentations at regional and national meetings. 3 publications are currently under preparation.

Publications (peer-reviewed):

1. Nance, J.; Bowman, D. N.; Mukherjee, S.; Kelley, C. T.; Jakubikova, E. Insights into the Spin-State Transitions in $[\text{Fe}(\text{tpy})_2]^{2+}$: Importance of the Terpyridine Rocking Motion *Inorg. Chem.* 2015, 54, 11259-11268.
2. Bowman, D. N.; Bondarev, A.; Mukherjee, S.; Jakubikova, E. Tuning the Electronic Structure of $\text{Fe}(\text{II})$ Polypyridines via Donor Atom and Ligand Scaffold Modifications: A Computational Study *Inorg. Chem.* 2015, 54, 8786-8793.
3. Mara, M. W.; Bowman, D. N.; Buyukcakir, O.; Shelby, M. L.; Haldrup, K.; Huang, J.; Harpham, M. R.; Stickrath, A. B.; Zhang, X.; Stoddart, J. F.; Coskun, A.; Jakubikova, E.; Chen, L. X. Electron Injection from Copper Diimine Sensitizers into TiO_2 : Structural Effects and Their Implications for Solar Energy Conversion Devices *J. Am. Chem. Soc.* 2015, 137, 9670-9684.
4. C. Liu, E. Jakubikova, Two-Step Model for Ultrafast Interfacial Electron Transfer: Limitations of Fermi's Golden Rule Revealed by Quantum Dynamics Simulations, *Chem. Sci.* 2017, 8, 5979-5991.
5. S. Mukherjee, D. E. Torres, E. Jakubikova, HOMO Inversion as a Strategy for Improving the Light Absorption Properties of $\text{Fe}(\text{II})$ Chromophores, *Chem. Sci.* 2017, 8, 8115-8126.
6. S. Mukherjee, C. Liu, E. Jakubikova, Comparison of Interfacial Electron Transfer Efficiency in $[\text{Fe}(\text{ctpy})_2]^{2+}$ - TiO_2 and $[\text{Fe}(\text{cCNC})_2]^{2+}$ - TiO_2 Assemblies: Importance of Conformational Sampling, *J. Phys. Chem. A* 2018, 122, 1821-1830.

Manuscripts in Preparation

1. S. Mukherjee, A. Bondarev, C. Liu, G. Van Den Drissche, E. Jakubikova, Tuning the Ligand Field Strength of $\text{Fe}(\text{II})$ -polypyridine Complexes, planned submission to *Inorg. Chem.*
2. D. C. Ashley, S. Mukherjee, E. Jakubikova, "Computational Design of Air-stable Cyclometalated $\text{Fe}(\text{II})$ Complexes," planned submission to *Inorg. Chem.*
3. C. Tichnell, J. Miller, C. Liu, S. Mukherjee, E. Jakubikova, J. K. McCusker, "Probing Electrolyte Modulation of $\text{Fe}(\text{II})$ (2,2'-bipyridine-4,4'-dicarboxylic acid) $_2(\text{CN})_2$ Sensitization of TiO_2 ," planned submission to *PCCP*.

Presentations at Universities and National Laboratories, given by Dr. Jakubikova

1. Argonne National Laboratory, 11/10/2015
2. UNC Chapel Hill, 3/1/2016
3. Texas Tech University, 5/10/2016
4. Rutgers University - Newark, 9/30/2016
5. University of New Mexico, 10/7/2016
6. Colgate University, 9/12/2017
7. University of North Texas at Denton, 9/22/2017
8. Florida State University, 2/7/2018
9. Los Alamos National Laboratory, 2/15/2018
10. University of New Mexico, 4/2/2018
11. Northeastern University, 4/18/2018

Invited oral presentations at conferences by Dr. Jakubikova

1. Workshop on Non-equilibrium Phenomena, Nonadiabatic Dynamics and Spectroscopy, Telluride, CO, 7/20/2015
2. 14th MERCURY Conference for Undergraduate Computational Chemistry, Bucknell University, PA, 7/25/2015
3. NC Photochem '15, Charlotte, NC, 10/10/2015
4. ACS National Meeting, San Diego, CA, 3/14/2016
5. SERMACS, Columbia, NC, 10/25/2016
6. I-APS meeting, Sarasota, FL, 1/3/2017
7. SETCA, Oxford, MS, 5/19/2017
8. ACS GLRM, Fargo, ND, 6/27/2017
9. TSRC workshop on Nanomaterials: Computation, Theory, and Experiment, Telluride, 7/15/2017

Contributed poster presentations at conferences by Dr. Jakubikova

RPPR Final Report as of 21-Sep-2018

1. ACS National Meeting, Boston, MA, 8/18/2015
2. GRC on Donor-Acceptor Interactions, Newport, RI, 8/7-12/2017

Student presentations (poster and oral)

Sriparna Mukherjee (graduate student, postdoctoral researcher)

1. NC Photochem '15, Charlotte, NC, 10/10/2015
2. SERC - UNC-CH, Chapel Hill, NC, 10/15/2015
3. NC ACS, 9/18/2015
4. SETCA (Southeast Theoretical Chemistry Association), 5/14/2016
5. SERMACS, Columbia, NC, 10/23-26/2016 (oral)
6. NC Photochem, Raleigh, NC, 10/1/2016
7. SERC, UNC Chapel Hill, NC, 10/20-21/2016
8. SERMACS, Charlotte, NC, 11/8/2017
9. 131st Local Section Conference of NC ACS, 11/17/2017

Chang Liu (graduate student)

1. NC Photochem '15, Charlotte, NC, 10/10/2015
2. NC ACS, 9/18/2015
3. SETCA, 5/14/2016
4. 24th CCTCC, Jackson, MS, 11/11/2016

Jessica Gonzalez-Delgado (graduate student)

1. NC Photochem, Raleigh, NC, 10/1/2016

David Torres (high school student)

1. SERMACS, Columbia, SC, 10/23-26/2016

Jason Brannock (undergraduate student)

1. SERMACS, Columbia, SC, 10/23-26/2016

Results Dissemination

Outreach

The Jakubikova lab hosted a high school student, David Torres, from Wake STEM Early College High School in her laboratory as a part of the AEOP High School Apprenticeship Program.

Dr. Jakubikova was a keynote speaker at North Carolina School of Science and Mathematics (NCSSM) on October 3, 2015. She gave a guest lecture on Computational Sciences addressing a group of approximately 70 high school students who take classes in computational science at NCSSM. As a part of the lecture, she discussed her work on developing Fe(II)-based chromophores for use in dye-sensitized solar cells.

Honors and Awards: Dr. Jakubikova has received NSF CAREER award in 2016. She has also obtained tenure at NCSU in August 2016.

Dr. Jakubikova was selected as one of the 16 emerging investigators in the areas of photochemistry and photophysics by Inorganic Chemistry journal, in December 2016. Two articles published in Inorganic Chemistry supported by this ARO grant were highlighted in the Inorganic Chemistry virtual issue: Inorg. Chem., 2015, 54 (17), pp 8786–8793, and Inorg. Chem., 2015, 54 (23), pp 11259–11268 (<http://pubs.acs.org/page/vi/photochemistry-photophysics>).

Students involved in this project also received various poster awards for their presentations and national and regional meetings, as described below:

1. Chang Liu, PhD student was awarded 3rd place in the Graduate Poster Presentation at the 24th Conference on Current Trends in Computational Chemistry (CCTCC) that took place on November 11-12, 2016, in Jackson, MS.
2. Jason Brannock (undergraduate student), and David Torres (high school student) both received an award for the best junior poster in their category from the Division of Computers in Chemistry at the Southeastern Regional Meeting of the American Chemical Society (SERMACS) in Columbia, SC on October 23-26, 2016.

Protocol Activity Status:

RPPR Final Report as of 21-Sep-2018

Technology Transfer: 1. We have started a collaboration with Drs. Ping Yang and Marc Cawkwell at Los Alamos National Laboratory, focusing on development of DFTB tools for simulation of Fe(II)-dye-nanoparticle assemblies. As a part of this collaboration, Chang Liu, a graduate student in the Jakubikova laboratory spent 2 months at LANL in 2016 (August and September) working on DFTB parameterization. The same student is currently spending another three months at LANL (June-August) with the aim to finish parameterization of Fe-C set for DFTB calculations.

2. Thanks to our expertise in the photochemistry of transition metal compounds, we have started a collaboration with Dr. Ryan O'Donnell at Army Research Laboratory, in which we provide computational support for a project focused on design of novel iridium based chromophores.

PARTICIPANTS:

Participant Type: PD/PI

Participant: Elena Jakubikova

Person Months Worked: 3.00

Funding Support:

Project Contribution:

International Collaboration:

International Travel:

National Academy Member: N

Other Collaborators:

Participant Type: Graduate Student (research assistant)

Participant: David Bowman

Person Months Worked: 2.00

Funding Support:

Project Contribution:

International Collaboration:

International Travel:

National Academy Member: N

Other Collaborators:

Participant Type: Graduate Student (research assistant)

Participant: Sriparna Mukherjee

Person Months Worked: 15.00

Funding Support:

Project Contribution:

International Collaboration:

International Travel:

National Academy Member: N

Other Collaborators:

Participant Type: Graduate Student (research assistant)

Participant: Chang Liu

Person Months Worked: 15.00

Funding Support:

Project Contribution:

International Collaboration:

International Travel:

National Academy Member: N

Other Collaborators:

Participant Type: Graduate Student (research assistant)

Participant: Jessica Gonzalez-Delgado

Person Months Worked: 6.00

Funding Support:

Project Contribution:

International Collaboration:

RPPR Final Report
as of 21-Sep-2018

International Travel:
National Academy Member: N
Other Collaborators:

Participant Type: Graduate Student (research assistant)

Participant: Hyuk-Yong Kwon

Person Months Worked: 1.00

Funding Support:

Project Contribution:

International Collaboration:

International Travel:

National Academy Member: N

Other Collaborators:

Participant Type: Postdoctoral (scholar, fellow or other postdoctoral position)

Participant: Sriparna Mukherjee

Person Months Worked: 9.00

Funding Support:

Project Contribution:

International Collaboration:

International Travel:

National Academy Member: N

Other Collaborators:

Participant Type: Postdoctoral (scholar, fellow or other postdoctoral position)

Participant: Daniel Charles Ashley

Person Months Worked: 4.00

Funding Support:

Project Contribution:

International Collaboration:

International Travel:

National Academy Member: N

Other Collaborators:

Participant Type: Undergraduate Student

Participant: Alexey Bondarev

Person Months Worked: 2.00

Funding Support:

Project Contribution:

International Collaboration:

International Travel:

National Academy Member: N

Other Collaborators:

Participant Type: Undergraduate Student

Participant: Jason Brannock

Person Months Worked: 3.00

Funding Support:

Project Contribution:

International Collaboration:

International Travel:

National Academy Member: N

Other Collaborators:

Participant Type: High School Student

Participant: David Esteban Torres

Person Months Worked: 4.00

Funding Support:

Project Contribution:

RPPR Final Report
as of 21-Sep-2018

International Collaboration:
International Travel:
National Academy Member: N
Other Collaborators:

DISSERTATIONS:

Publication Type: Thesis or Dissertation

Institution:

Date Received: 26-Oct-2015

Completion Date:

Title: Earth-Abundant Sensitizers for Solar Energy Capture: Developing a Practical Computational Approach

Authors:

Acknowledged Federal Support:

Publication Type: Thesis or Dissertation

Institution: North Carolina State University

Date Received: 31-Aug-2017

Completion Date: 8/28/17 4:56PM

Title: Solar Energy Harvesting with Fe(II)-polypyridines: Strategies for Tuning Light Absorption and Interfacial Electron Transfer

Authors: Sriparna, Mukherjee

Acknowledged Federal Support: **Y**

Publication Type: Thesis or Dissertation

Institution: North Carolina State University

Date Received: 13-Jul-2018

Completion Date: 9/9/17 1:34AM

Title: Metal Polypyridine Sensitizers for Dye-Sensitized Solar Cells: Computational Studies of Interfacial Electron Transfer Dynamics

Authors: Jessica, Gonzalez-Delgado

Acknowledged Federal Support: **Y**

Accomplishments (May 1, 2015 – April 30, 2018)

This report summarizes our results obtained for each of the specific objectives of the proposal: (1) increasing the lifetime of metal-to-ligand charge transfer (MLCT) states, (2) optimization of the absorption properties of Fe(II)-polypyridines, and (3) speeding up the rate of the interfacial electron transfer (IET) between the excited chromophore and semiconductor. Outline of the major activities and significant results is provided below.

1. Key Outcomes

In summary, we determined that the ligand field strength (LFS) of Fe(II) complexes can be predominantly tuned via the σ -bonding interactions, and that the presence of Fe-C bonds results in the strongest LFS out of the complexes investigated.¹⁻² We further determined that substitutions of strongly electron withdrawing groups, such as NO₂, stabilize Fe complexes with aryl ligands in Fe(II) oxidation state in air. (Objective 1)

Second, we found that light-absorption properties of Fe(II)-polypyridines can be tuned via the substitution of π -conjugated electron donor groups onto the polypyridine scaffold, creating complexes with “inverted HOMO” character (with the HOMO localized on the ligand rather than the metal center), and a dramatic improvement in the light absorption properties.³ (Objective 2)

Finally, we identified a number of structure-property relationships in dye-semiconductor assemblies responsible for tuning the rate of interfacial electron transfer (IET).⁴⁻⁶ Most importantly, *we have established the importance of conformational sampling for modeling the IET and put together a reliable computational protocol for calculating IET rates and internal quantum efficiencies.*⁷ Finally, ***we determined the mechanism of interfacial electron transfer (IET) at dye-semiconductor interfaces*** and established the limitations of Fermi’s golden rule for description of the overall rate of the IET.⁸ We have also applied this knowledge to explain dependence of IET rates in the presence of various additives based on tert-butylpyridine in DSSCs. (Objective 3)

2. Activities, Specific Objectives, and Significant Results

Major activities for the 3-year period are summarized below.

2.A Objective 1: Increasing the Lifetime of the MLCT states

Major Activities

The major activities related to this objective centered on the systematic computational studies of a series of complexes based on [Fe(dcpp)₂]²⁺ (dcpp = 2,6-bis(2-carboxypyridyl)pyridine) and [Fe(tpy)₂]²⁺ (tpy = 2,2':6',2''-terpyridine) as shown in Figure 1.

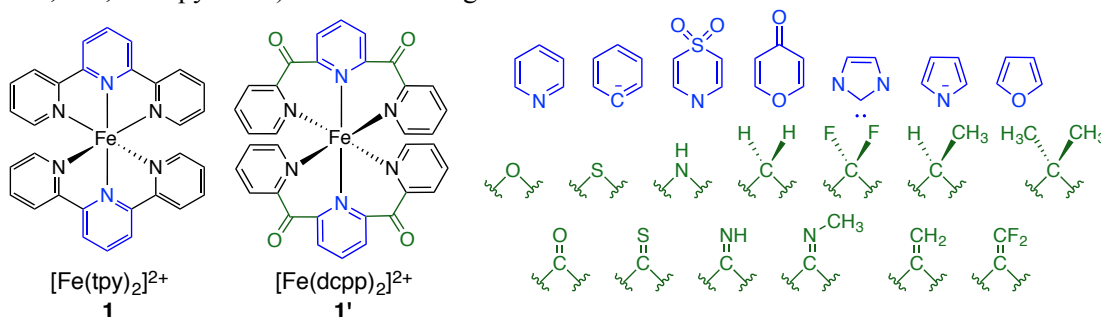


Figure 1. Series of [Fe(tpy)₂]²⁺ and [Fe(dcpp)₂]²⁺ based complexes investigated in this study. The first series (in blue) investigated the impact of the donor atom character (C, N, O) on the ligand field strength of the iron complexes. The second series (in green) was design to investigate the influence of pyridine linking on the ligand field strength.

Specific Objectives

The $[\text{Fe}(\text{dcp})_2]^{2+}$ complex was synthesized and characterized by McCusker and coworkers in 2014,⁹ suggesting that it possesses significantly increased ligand field strength relative to prototypical Fe(II)-polypyridine complexes, such as $[\text{Fe}(\text{tpy})_2]^{2+}$ and $[\text{Fe}(\text{bpy})_3]^{2+}$. The goal of our systematic studies was to determine the role played by the identity of the donor atom and pyridine linking group in increasing the ligand field strength in Fe(II) complexes and formulate rational strategies for ligand design that would help us to increase the ligand field strength to the point where the ordering of metal-centered states is $^1\text{A}_1 < ^3\text{T}_1 < ^3\text{T}_2 < ^1\text{T}_1 < ^5\text{T}_2$ (see Tanabe-Sugano diagram in Figure 2), and metal-to-ligand charge transfer states will be the lowest energy excited states in the complex.

Significant Results

We have performed density functional theory (DFT) calculations at the B3LYP+D2/6-311G* level of theory to evaluate how the ligand field strength of Fe(II) complexes derived from $[\text{Fe}(\text{dcp})_2]^{2+}$ and $[\text{Fe}(\text{tpy})_2]^{2+}$ changes with the donor atom substitutions (Figure 1, series in blue) as well as with the changes in the character of the pyridine linking group (Figure 1, series in green).

Modification of the first coordination sphere of Fe(II) complexes: For the series with systematic changes in the first coordination sphere (i.e., changes in the identity of the donor atom), we found that the use of a dcpp scaffold allows for a significant increase of the ligand field strength of Fe(II) complexes as well as a more ideal octahedral coordination environment compared to the tpy scaffold. Additionally, we found a clear trend in the effect of the donor atom identity on the resulting ligand field strength (see Figure 3). The N-heterocyclic carbene and aryl ring, both with a C donor atom, provide for the strongest ligand fields regardless of the ligand scaffold. Nitrogenous heterocyclic rings provide for moderate ligand field strength, while oxygen-based heterocycles result in the weakest field strength. Based on these studies, for applications of Fe(II) polypyridines as chromophores, the following design criteria seem to be of upmost importance: (1) presence of Fe–C bonds in the system, (2) ideal octahedral environment, and (3) short metal-ligand bond lengths. The results of this work were published in *Inorganic Chemistry* in 2015.¹

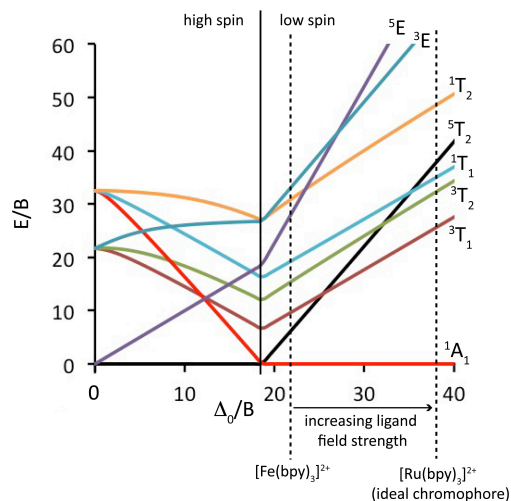


Figure 2. Simplified Tanabe-Sugano diagram for an octahedral d^6 complex with O_h symmetry. Δ_0 corresponds to the ligand field splitting parameters, and E denotes the energy. Note that the order of the various electronic states ($^1\text{A}_1$, $^3\text{T}_1$, $^1\text{T}_1$, $^5\text{T}_2$) changes depending on the value of the ligand field splitting parameter.

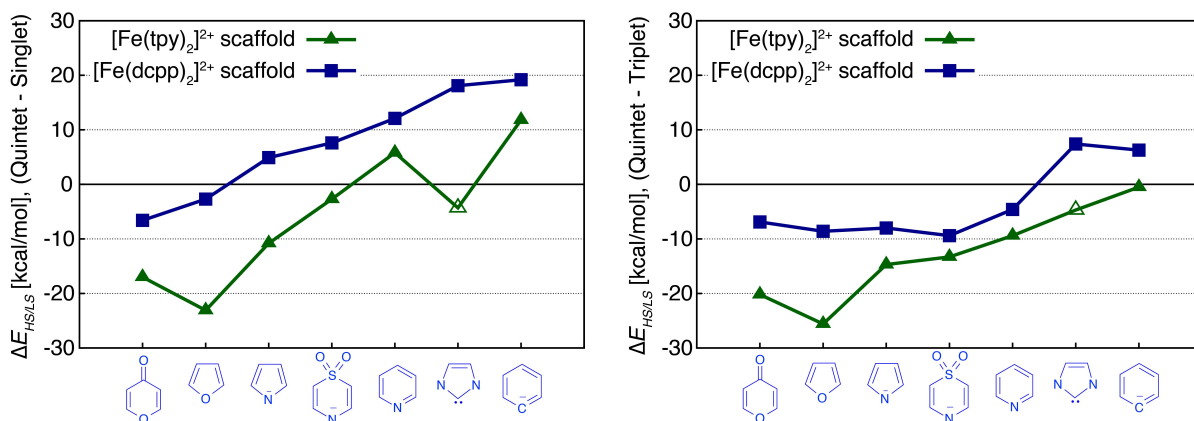


Figure 3. Plot of $\Delta E_{\text{HS/LS}}$ between the quintet and singlet states (left) and quintet and triplet states (right) for the $[\text{Fe}(\text{tpy})_2]^{2+}$ (green line) and $[\text{Fe}(\text{dcp})_2]^{2+}$ (blue line) based complexes versus the identity of the central ring.

While our studies have predicted that Fe(II) compounds with aryl ligands will have improved ligand field strength in comparison to the pyridine ligands (see Figure 3), experimental reports of such complexes are lacking. In 2017, synthesis of an Fe(III) complex with an NCN ligand (NCHN = 1,3-di(pyridin-2-yl)benzene) was reported.¹⁰ The report suggested that while Fe(II) complex is initially formed, it is not stable in air, oxidizing to Fe(III) in the presence of oxygen. Based on this, we have suggested that it is possible to stabilize $[\text{Fe}(\text{NCN})_2]^{2+}$ in Fe(II) oxidation state by substituting a strongly electron withdrawing group, such as NO_2 to the ligand scaffold. Table 1 summarizes the calculated ligand field strength ($\Delta E_{\text{Q/S}}$ = Energy of quintet – Energy of singlet), Fe(II/III) redox potentials for the three complexes, as well as ΔG_{O_2} defined Gibbs free energy for outer sphere electron transfer between the Fe(II) complexes and O_2 :

$$\Delta G_{\text{O}_2} = -\frac{[E_{\text{O}_2}^{1/2} - E_{\text{Fe}}^{1/2}]}{nF}$$

where $E_{\text{O}_2}^{1/2}$ is the redox potential of O_2 , and $E_{\text{Fe}}^{1/2}$ is the redox potential for Fe(II/III) couple.

Table 1. Calculated redox potentials, Gibbs free energy and quintet-singlet energy gaps for a series of Fe(II) complexes. Structure optimized and $\Delta E_{\text{Q/S}}$ calculated at the B3LYP+D2/SDD(Fe),6-311G* level of theory

Complex	$E^{1/2}(\text{Fe}^{\text{II/III}})$ vs. NHE [V]	ΔG_{O_2} [kcal/mol]	$\Delta E_{\text{Q/S}}$ [kcal/mol]
$[\text{Fe}(\text{tpy})_2]^{2+}$	1.47	38.01	4.4
$[\text{Fe}(\text{NCN})_2]^{2+}$	-0.18	0.08	10.6
$[\text{Fe}(\text{NCN-NO}_2)_2]^{2+}$	0.51	15.82	13.5

As can be seen in Table 1, changing two pyridine ligands to aryls (going from $[\text{Fe}(\text{tpy})_2]^{2+}$ to $[\text{Fe}(\text{NCN})_2]^{2+}$, dramatically changes the oxidation potential of the Fe(II) center, making it easy to oxidize in the presence of oxygen, as evidenced by the Gibbs free energy for the redox reaction being ~ 0 kcal/mol. Substitution of the $-\text{NO}_2$ groups onto the 4 positions of the aryl ring (see complex $[\text{Fe}(\text{NCN-NO}_2)_2]^{2+}$) stabilizes the Fe(II) center in the presence of oxygen making it more difficult to oxidize. At the same time, both $[\text{Fe}(\text{NCN})_2]^{2+}$, and $[\text{Fe}(\text{NCN-NO}_2)_2]^{2+}$ complexes have a stronger ligand field strength than the $[\text{Fe}(\text{tpy})_2]^{2+}$ complex. Substitution by the electron withdrawing groups therefore provides a viable strategy for preparation of air-stable cyclometalated Fe(II) complexes. At the same time, redox potential of Fe(II/III) couple was identified as an important design criterion for Fe(II) chromophores.

Modification of the second coordination sphere of Fe(II) complexes:

Systematic modifications of the second coordination sphere (i.e., identity of the pyridine linker group) were shown to have appreciable impact on the ligand field strength of the complexes. The CO linking group provides for the strongest ligand field strength, while $\text{C}(\text{CH}_3)_2$ linker results in a complex with the weakest ligand field strength. Several of the investigated complexes display stronger ligand field strength in comparison to the $[\text{Fe}(\text{tpy})_2]^{2+}$ parent complex (see Figure 4). Both steric and electronic effects are responsible for the

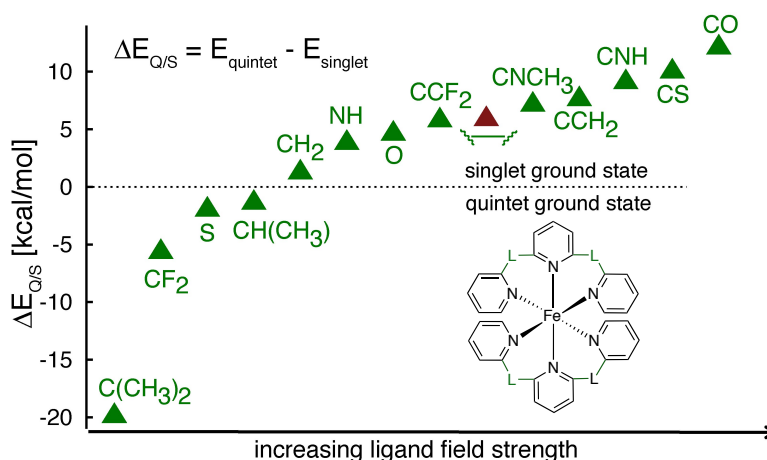


Figure 4. Plot of $\Delta E_{\text{HS/LS}}$ between the quintet and singlet states for the $[\text{Fe}(\text{dcpp})_2]^{2+}$ (blue line) based complexes versus the identity of the linking group.

observed behavior. The key structural factors that impact the ligand field strength in these complexes are: (1) hybridization of the connecting atom (sp^2 vs. sp^3), (2) van der Waals volume of the linking group, and (3) iron-nitrogen bond length. The linking groups with a larger van der Waals volume cause an increase in the Fe-N bond length and subsequent decrease of the ligand field strength. The sp^2 hybridized connecting groups yield complexes with stronger ligand field strength than the sp^3 hybridized linking groups (see Figure 5).

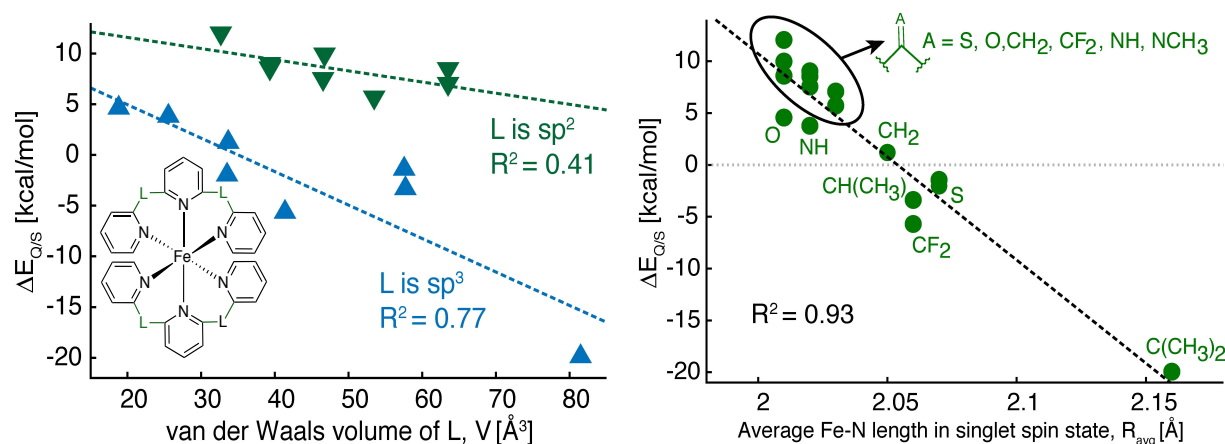


Figure 6. Dependence of ligand field strength on the van der Waals volume of the linking group (left) and Fe-N distance (right).

2.B Objective 2: Optimization of the Absorption Properties of Fe(II)-polypyridines

Activities

The goal of these studies was to investigate the light-harvesting properties of a series of Fe(II)-polypyridine complexes that incorporate push-pull design into the same ligand. Both ground state electronic structure (MO energies, HOMO-LUMO gaps, and percent of electron density on the carboxylic acid linker group) and excited state properties (UV-Vis absorption spectra) were calculated for a series of dyes shown in Figure 6.

Motivation and Specific Objectives

Heteroleptic push-pull ligand design is commonly used to optimize light-harvesting properties and increase the IET efficiency of Ru(II)-polypyridine sensitizers for DSSCs.¹¹ Our objective was to apply the same principles in the ligand design of Fe(II)-polypyridines. Due to practical difficulties with the synthesis of heteroleptic Fe(II) complexes, we have created a series of homoleptic complexes that incorporate push-pull characteristics into one ligand. Investigated Fe(II) complexes were then evaluated for their capability to absorb visible light as well as the ground state properties indicative of a possible increase of the IET rate in dye-semiconductor assemblies.

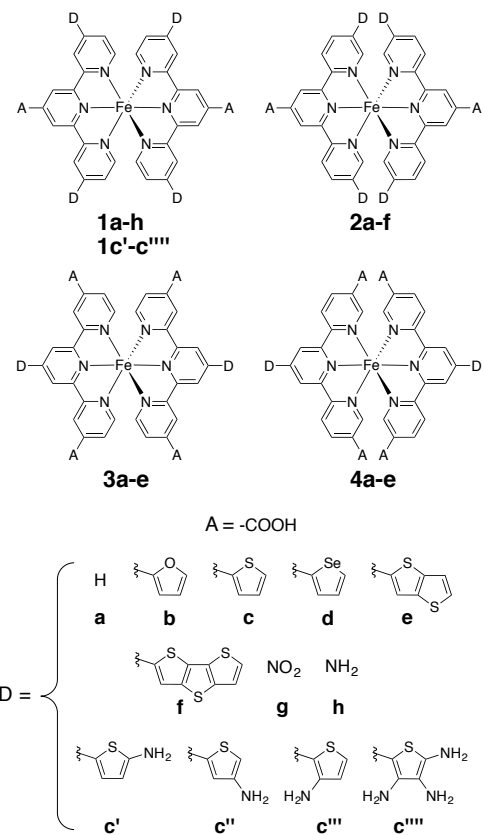


Figure 5. Fe(II) complexes investigated with the aim to improve the absorption properties of Fe(II)-polypyridines. Note that **1a** and **2a** are identical.

Significant Results

All structures were optimized at the B3LYP+D2/6-311G* level of theory in water (solvent included via a polarizable continuum model). The ground state electronic structure of each complex was analyzed to obtain the information on HOMO-LUMO gaps of each complex, as well as percent of electron density on the carboxylic acid group. The HOMO-LUMO gaps in general correlate with the wavelength at which the complex absorbs light (the smaller the HOMO-LUMO gap, the lower the absorption wavelength), while the % of electron density on the linker group correlates with the speed of the IET between the excited dye and the conduction band of TiO₂.¹²

One of the most important results we found was a significant decrease in the HOMO-LUMO gap (~ 0.5 eV) upon the substitution of donor groups. Selenophene (**d**) provides for the smallest decrease, while tritriophene (**f**) provides for the largest decrease of the HOMO-LUMO gap (see Figure 7). This suggests that absorption profile of these complexes should be shifted toward the red relative to the parent [Fe(tpy)₂]²⁺ complex. Moreover, the reduction in the HOMO-LUMO gap is due to the increase of the HOMO energy, while the energy of the LUMO stays virtually constant. This is important, since the LUMO energy is related to the driving force for the IET in dye-semiconductor assemblies and a significant decrease of the LUMO energy would negatively impact electron injection from the excited dye into TiO₂.

We have also found that it is more advantageous to place the electron withdrawing carboxylic acid group onto 4' position of the terpyridine scaffold rather than at 4 and 4" positions. Placement of two carboxylic acid groups onto the same ligand at 4 and 4" positions causes a substantial drop in the percent of electron density on the carboxylic acid group which has a negative impact on the IET rate between the excited dye and TiO₂ semiconductor.

The calculated UV-Vis absorption spectra for complexes **1a**, **1c**, **1e**, and **1f** are shown in Figure 8 along with the character of transitions with significant oscillator strength ($f_{osc} \geq 0.01$) in the visible region ($\lambda \geq 350$ nm). Transitions were classified as metal-centered (MC), metal-to-ligand charge transfer (MLCT), intra-ligand charge transfer (ILCT), or ligand-centered (LC) based on visual inspection. Mixed character was observed for several transitions; most of these displayed features of both MLCT and ILCT character.

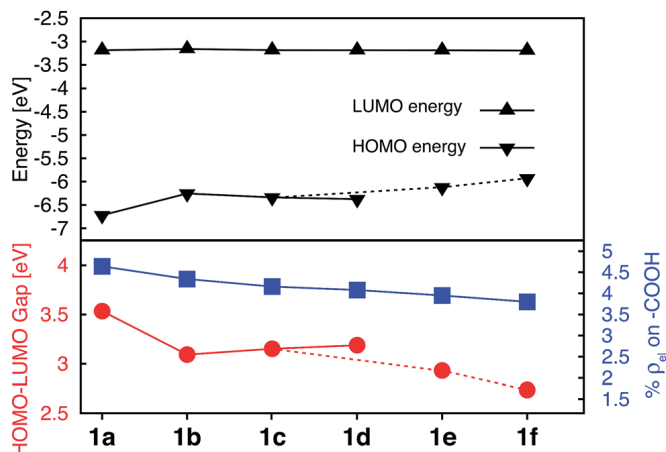


Figure 7. Electronic properties of **1a-f** series of complexes. Top: HOMO and LUMO energies. Bottom: HOMO-LUMO gaps (red) and average percent of electron density on the carboxylic acid in doubly degenerate LUMO (blue).

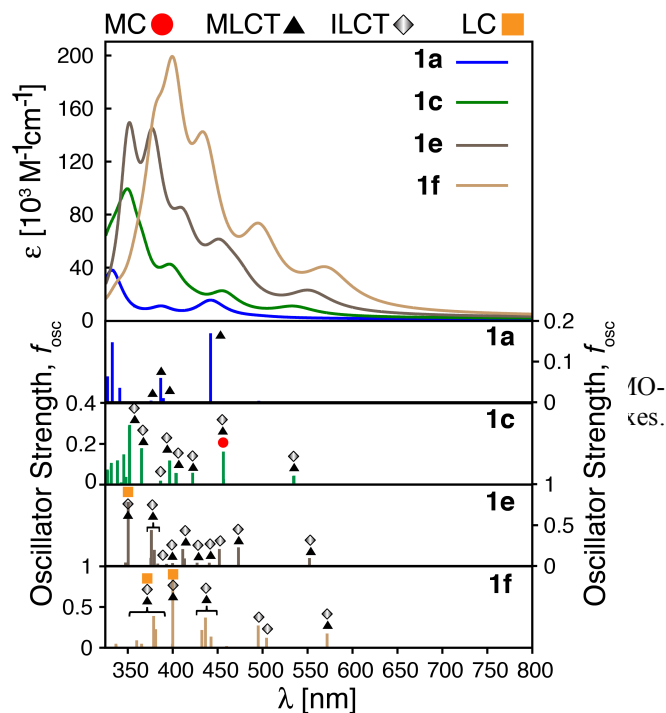


Figure 8. Top: Calculated UV-Vis spectra for complexes **1a**, **1c**, **1e** and **1f**. Bottom: Assignments for transitions with $\lambda \geq 350$ nm and oscillator strength $f_{osc} \geq 0.01$ for complexes **1a**, **1c**, **1e** and **1f**. MC: metal-centered, MLCT: metal-to-ligand charge transfer, ILCT: intra-ligand charge transfer and LC: ligand-centered.

Calculated UV-Vis spectra predict remarkable improvements in the absorption properties upon substitution of the tpy ligand by donor groups. The absorption spectra of substituted complexes shift towards lower energies, with most of their transitions displaying a mixed MLCT/ILCT character (compare transition assignments for **1c** vs. **1a**, see Figure 8). The substituted complexes also display significant increase in the molar absorptivity (see Figure 8). Extending the π -conjugation of the substituent groups (going from **1c** to **1e** and **1f**) further enhances the intensity as well as red shifts the spectrum. New transitions with pure ILCT character are also observed for complexes **1e** and **1f**. The improvements in the molar absorptivity are due to (1) an increased number of transitions in the lower energy region of the spectrum, and (2) mixed character (MLCT/ILCT) of these transitions.

Results of this work were published as an edge article in Chemical Science in 2017.³

3.C Objective 3: Speeding up the Rate of IET between the Excited Chromophore and Semiconductor

Activities

Activities were performed under this objective: (1) Evaluation of the impact of conformational flexibility of the dyes on the IET rate in dye-semiconductor assemblies. (2) Determination of structure-property relationships that impact IET rates. (3) Establishment of a reliable computational protocol for modeling IET in dye-semiconductor assemblies.

3.C.1. Impact of ligand conformation on the IET in dye-TiO₂ assemblies and identification of structural and electronic factors that impact IET rates

Motivation and Specific Objectives

Our previous studies of quantum dynamics of IET in Fe(II)-polypyridine-TiO₂ assemblies were always performed at a frozen structure obtained by DFT optimization at 0 K.^{6, 12-13} Measurements of the IET rates, however, occur at the room temperature at which the dyes can sample a number of different conformations. The goal of this work was twofold: First, to find out how does the structure of the dye at the moment of excitation impact the IET dynamics. Second, to identify structural and electronic factors that impact the speed of the IET and can be tuned via a ligand design.

Significant Results

We have performed quantum dynamics simulations to study IET in a prototype isonicotinic acid – TiO₂ assembly (see Figure 9). Isonicotinic acid (pyCA) is a model for carboxylated pyridyl rings which are common binding motifs for a variety of metal polypyridine dyes,² thus a detailed understanding of this system can be used to assist in rational design of efficient dye sensitizers. First, we investigated how different attachment modes of the linker on the surface (monodentate vs. bidentate), and distribution of adsorbate conformations at room temperature affects the IET. Second, we evaluated dependence of the calculated IET rates on various properties of the semiconductor and adsorbate featured in eq. (1) (i.e., electronic coupling, density of acceptor states on

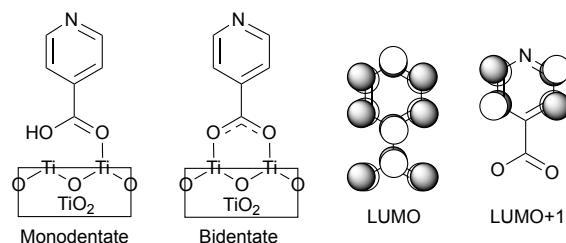


Figure 9. Model system for this work. **Left:** pyCA–TiO₂ semiconductor assemblies with monodentate and bidentate attaching mode. **Right:** nodal structure for LUMO and LUMO+1 of pyCA.

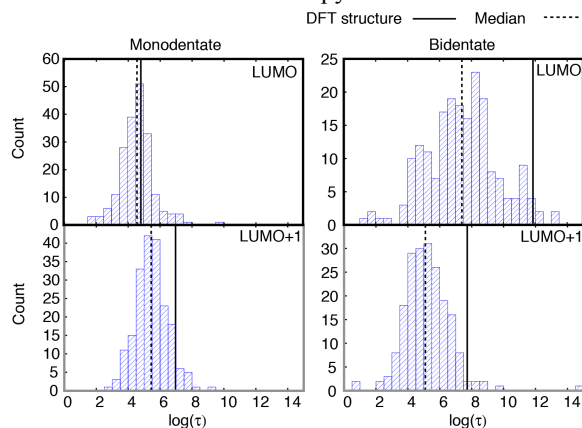


Figure 10. Log of characteristic IET time obtained for all sampled structures. Solid line denotes the characteristic time obtained for the DFT-optimized structure, while the dashed line denotes the median characteristic time for all sampled structures.

semiconductor, and driving force), thus gaining insight into the validity of Fermi's golden rule for theoretical description of the IET process.

The results of IET simulations showing the importance of conformational sampling along with a new, 2-step model of interfacial electron transfer. Figure 10 illustrates the distribution of IET rates obtained for 400 sampled structures at room temperature, 200 for monodentate and 200 for bidentate attachment. Note that for each attachment mode, DFTB+ with mio and tiorg parameter set was employed to run ten independent MD trajectories at room temperature for 42 ps with 1 fs time step (12 ps dephasing, 30 ps production run). Two hundred structures were randomly selected from the 10 independent runs for each attachment model. Interestingly, the conformational flexibility of the dye on the surface tends to speed up the IET rate. The effect is more apparent for the dye-TiO₂ assembly with a bidentate attachment mode. Another important point is that a particular structure of the dye at the time of photoexcitation can modulate the rate of the IET over several orders of magnitude! This suggests that to properly model the IET at dye-semiconductor assemblies, looking at a distribution of the calculated IET rates is important for full understanding of the system. This also has important implications for the interpretation of the experimentally-measured IET rates. Rather than measuring a single rate, the results of experimental measurements reflect a range of IET rates from an ensemble of molecules attached on the surface.

Next, we have investigated dependence of the calculated IET initial and overall characteristic times on various structural and electronic parameters of the system, which included energy of the initially populated orbitals (LUMO and LUMO+1), density of the available TiO₂ states at the energy of the initial wavepacket, Ti-O distance, dihedral angle between the pyridine ring and carboxylic acid linker, and energy difference between the energy of initially occupied MO and the edge of the conduction band of TiO₂. Lasso statistical analysis was utilized to identify parameters that have the largest impact on the initial and overall IET characteristic time (see Figure 11). Interestingly, the two most important electronic factors that impact the IET rate are the percent of electron density on the linker group which anchors the dye to TiO₂ (% ρ_{linker}), and the number of available TiO₂ acceptor states (ρ_{acceptor}). Figure 12 illustrates the strong relationship between these two parameters and initial characteristic time for IET. The IET occurs most efficiently for cases where both of these properties maximize their values. Both of these parameters can be obtained from relatively simple electronic structure calculations and therefore provide a

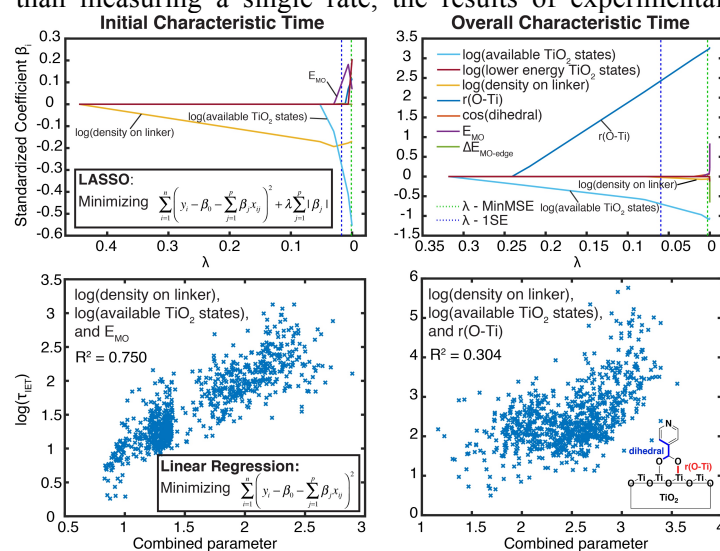


Figure 11. Lasso analysis and multiparameter regression identifying the parameters with the most impact on the initial and overall characteristic time. (τ_{IET} = characteristic time).

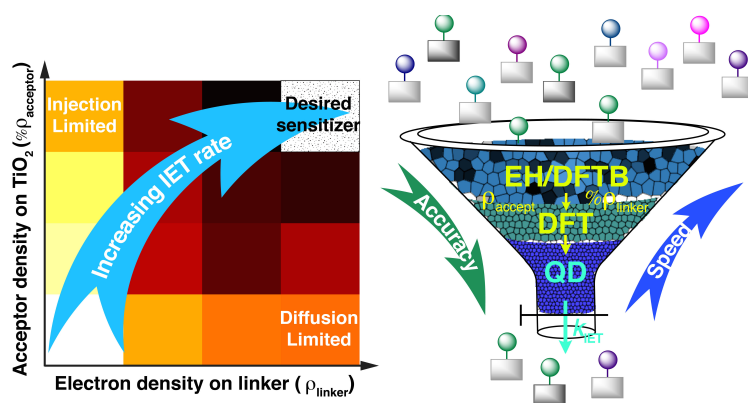


Figure 11. Left: Relationship between % ρ_{linker} , ρ_{acceptor} , and τ_{ini} . τ_{ini} is represented by a color value (darker = more efficient). Both variables are normalized by setting the new variable equal to: $x' = (x - x_{\text{min}})/(x_{\text{max}} - x_{\text{min}})$. Right: Suggested screening process for dye-sensitizers.

pathway to screening a large number of dye-nanoparticle assemblies that would exhibit a fast IET into the semiconductor.

Finally, based on these simulations we have proposed a two-step mechanism for the IET process in dye-TiO₂ assemblies (see Figure 13). The first step consists of the wavepacket injection from the dye into the TiO₂ nanoparticle. The second step is the diffusion of the wavepacket throughout the TiO₂ nanoparticle. We have identified two limiting cases of the IET transfer: a diffusion dominated case, and injection dominated case. For the diffusion dominated case, bottleneck for the efficient IET is the diffusion of the wavepacket inside the TiO₂ nanoparticle. It is further characterized by the initial IET rate being much faster than the overall IET rate, high electron density on the carboxylic acid linker group and energy levels of the initially populated excited states of the dye at the edge of the TiO₂ conduction band. On the other hand, initial electron injection from the excited dye into the TiO₂ nanoparticle is the bottleneck for the injection dominated case. Additionally, it is described by the initial IET rate being approximately the same as the overall IET rate, low electron density on the carboxylic acid linker and dye energy levels high in the TiO₂ conduction band. Fundamental understanding of the electron injection process in dye-semiconductor assemblies gained from these computational studies will enable us to formulate strategies for rational design of assemblies with improved electron injection efficiencies.

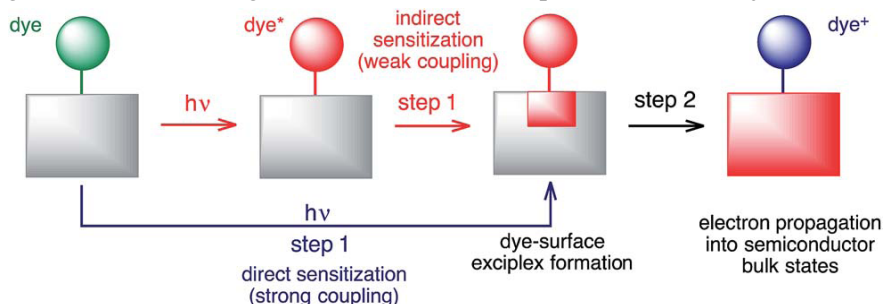


Figure 13. Schematic of the proposed 2-step model for IET.

Results of this work were published in Chemical Science in 2017.⁸

3.C.2. Computational Protocol for Modeling IET in Dye-Semiconductor Assemblies

As illustrated above, IET in dye-semiconductor systems is a complex process that is influenced by many factors, such as conformation of the dye at the moment of excitation and the attachment mode of the dye. Putting together what we have learned over the past few years about modeling such systems, we have established a computational protocol for modeling IET in dye-semiconductor systems that is capable of extracting wavelength-dependent internal quantum efficiencies from relatively straightforward atomistic simulations. It is expected that this protocol will change and get more refined in time as our understanding will advance, but this is explained here as a starting point for anyone aiming to perform IET simulations. The main features of the algorithm were published recently,⁷ and are briefly outlined below.

Step 1: Optimize structure at 0 K. Use a DFT approach to obtain structure of [Fe(tpy)₂]²⁺-TiO₂ assembly. Detailed description of our procedure for this step can be found in reference 6. In principle, any DFT or DFTB approach can be employed that provides a reliable structure of the dye and the semiconductor surface.

Step 2: Obtain a set of random dye conformations. This step can be performed either at the DFT or, more realistically due to large size of the system, at the DFTB level of theory. Ideally, one would perform MD simulations in the NVT ensemble for the entire dye-semiconductor assembly. If the size of the system or the lack of DFTB parameters represents a problem, obtaining MD trajectory of the dye with the linker fixed at the surface-optimized structure will be sufficient. A set of conformations will then be randomly selected from the MD trajectory run. The more samples are selected, the more accurate and

complete picture will be obtained at the end. Ideally, one would select ~ 100 structures to obtain a reliable set of data, but a selection of at least 10 sampled structures is recommended.

Step 3: Obtain absorption spectra of sampled structures. For each selected dye conformation, calculate UV-Vis spectra utilizing an excited state method. TD-DFT with a functional benchmarked for the dye selected will be sufficient. Determine excitations in the visible region ($\lambda > 350$ nm) with sufficient oscillator strength ($f > 0.01$) that will serve as initial states for the IET simulations. The cutoffs for λ and f may be adjusted based on the system investigated.

Step 4: Construct initial states for IET simulations. Initial states will be constructed as a linear combination of virtual orbitals that contribute to the particle states of the excited state at a particular wavelength λ , with the coefficients determined from the calculated transition densities:

$$|\psi_\lambda(0)\rangle = \frac{\sum_i a_i^2 |\text{LUMO}+i\rangle}{\sum_i a_i^2}$$

Note that in our model, we employ wavepacket dynamics approach developed by Batista and coworkers to propagate the initial state in time,¹⁴ which employs an extended Huckel (EH) Hamiltonian. Therefore, at this step it is important to compare MOs obtained from DFT calculations to the MOs obtained from EH calculations and, if necessary, optimize EH parameters to match the orbital shapes obtained from DFT.

Step 5: Propagate wavepacket in time:¹⁴

$$|\Psi_\lambda(t)\rangle = e^{-(i/\hbar)\hat{H}t} |\Psi_\lambda(0)\rangle = \sum_i B_i(t) |\chi_i\rangle$$

and obtain survival probabilities:

$$P_\lambda(t) = \left| \sum_i \sum_j^{dye\ all} B_i^*(t) B_j(t) S_{ij} \right| \in [0,1]$$

In this calculation step, simulations are done for each dye-nanoparticle assembly (each sampled structure) for each excited state identified from TD-DFT calculations.

Step 6: Obtain characteristic time for IET and average rate. To obtain the characteristic time (i.e., time at which 50% of the wavepacket is injected into the nanoparticle), we fit survival probability with a multi-exponential function:

$$P_\lambda(t) = \sum_{i=1}^N C_i e^{-\alpha_i t}, \quad N = 1, 2, 3$$

with the constraint $P_\lambda(0)=1$ that is satisfied by $\sum_{i=1}^N C_i = 1$ ($N = 1, 2, 3$). In our experience, single or double exponential fit usually sufficient (i.e., with the survival probability with $R^2 > 0.95$), with very few generated survival probability functions requiring a triple exponential fit. The characteristic time at a specific wavelength, $\tau_{\text{IET}}(\lambda)$, was calculated from the expectation value of the survival probability given by

$$\tau_{\text{IET}}(\lambda) = \frac{\int_0^\infty t P_\lambda(t) dt}{\int_0^\infty P_\lambda(t) dt}$$

Step 7: Obtain theoretical internal quantum efficiency (TIQE). The TIQE at a given wavelength $\text{TIQE}(\lambda)$ can be obtained as⁴

$$\text{TIQE}(\lambda) = \frac{k_{\text{IET}}(\lambda)}{k_{\text{IET}}(\lambda) + k_{\text{ISC}}}$$

where $k_{\text{IET}}(\lambda) = [\tau_{\text{IET}}(\lambda)]^{-1}$, in which k_{ISC} is experimentally-determined rate of intersystem crossing that competes with the IET process and $k_{\text{IET}}(\lambda) = [\tau_{\text{IET}}(\lambda)]^{-1}$. The distribution of TIQEs obtained from all sampled conformations of the dye can then be plotted as histogram by averaging over 10 nm intervals starting from 350 nm.

There are several important features incorporated in our computational protocol. First, instead of a single, fully optimized conformation of the dye at 0 K, we suggest the use of a range of conformations to obtain a distribution of rates. An inclusion of conformational sampling into the model can dramatically change the predicted IET efficiencies, independently of the theoretical approaches utilized. Second, it is important to model the initial state based on TD-DFT calculations rather than on orbital-by-orbital basis, to obtain the wavelength-dependence in our calculated IET rates. Finally, while computational approaches based on Fermi's golden rule framework provide excellent first insights into the interfacial properties and are usually good predictors of the initial IET rates, they do not necessarily correlate with the overall IET rates.⁸ Therefore, utilization of time-dependent approaches for IET simulations is highly recommended.

While the suggested computational protocol presents a substantial improvement over the current state-of-art, it can still be developed further and improved. Some obvious targets for improvement are (1) inclusion of explicit solvent into the simulations, and (2) explicit coupling of quantum dynamics and molecular dynamics simulations.

3.C.3. IET modeling of $[\text{Fe}(\text{dcbpy})_2(\text{CN})_2]^{2+}$ on TiO_2 (collaboration with Prof. McCusker, MSU)

The computational protocol described above was applied to model $[\text{Fe}(\text{dcbpy})_2(\text{CN})_2]^{2+}$ on TiO_2 , specifically looking at the dependence of IET in the presence of various additives. In the absence of the additives, the LUMO of the $[\text{Fe}(\text{dcbpy})_2(\text{CN})_2]^{2+}$ dye lies approximately 0.4 eV above the edge of the TiO_2 conduction band (CB). In the presence of tert-butyl pyridine (t-BuPy) and di-tert-butyl pyridine (d-tBuPy), the CB of TiO_2 is shifted, changing the energy difference between the LUMO of the dye and TiO_2 CB to 0.4 eV and 0.3 eV, respectively. This change in the alignment between the energy levels of the Fe(II) dye and the TiO_2 conduction band, results in significant changes in the calculated TIQEs for the lower energy absorption band, as seen in Figure 14. This suggests that solar cells that contain dyes that inject from initially-excited states with very short (sub-picosecond) lifetimes (such as Fe(II)-polypyridines), are very sensitive to the environment and it is important to pay attention to these factors when optimizing the function of Fe(II)-sensitized solar cells.

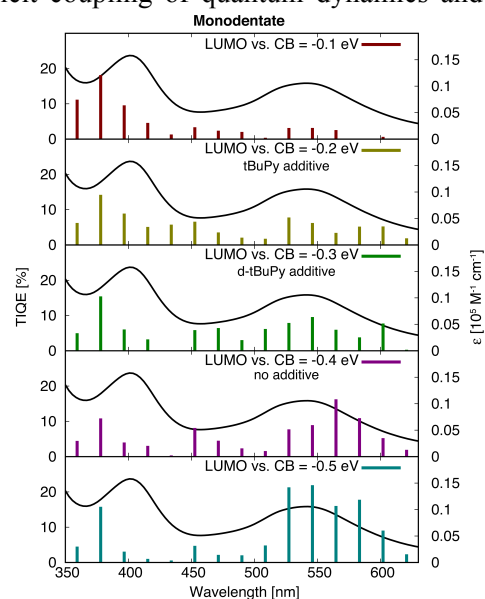


Figure 14. Theoretical quantum efficiency (sticks) for different alignments of the LUMO of the dye and the CB edge of TiO_2 .

4. References

1. Bowman, D. N.; Bondarev, A.; Mukherjee, S.; Jakubikova, E., Tuning the Electronic Structure of Fe(II) Polypyridines via Donor Atom and Ligand Scaffold Modifications: A Computational Study. *Inorg. Chem.* **2015**, *54* (17), 8786-8793.
2. Mukherjee, S.; Bowman, D. N.; Jakubikova, E., Cyclometalated Fe(II) complexes as sensitizers in dye-sensitized solar cells. *Inorg. Chem.* **2015**, *54* (2), 560-569.

3. Mukherjee, S.; Torres, D. E.; Jakubikova, E., HOMO inversion as a strategy for improving the light-absorption properties of Fe(II) chromophores. *Chem. Sci.* **2017**, 8 (12), 8115-8126.
4. Bowman, D. N.; Mukherjee, S.; Barnes, L. J.; Jakubikova, E., Linker dependence of interfacial electron transfer rates in Fe(II)-polypyridine sensitized solar cells. *J. Phys. Condens. Matt.* **2015**, 27 (13), 134205.
5. Bowman, D. N.; Chan, J.; Jakubikova, E., Investigating interfacial electron transfer in highly efficient porphyrin-sensitized solar cells. In *Surface Chemistry for Photocatalysis*, Kilin, D. S., Ed. 2015.
6. Bowman, D. N.; Blew, J. H.; Tsuchiya, T.; Jakubikova, E., Elucidating Band-Selective Sensitization in Iron(II) Polypyridine-TiO₂ Assemblies. *Inorg. Chem.* **2013**, 52 (15), 8621-8628.
7. Mukherjee, S.; Liu, C.; Jakubikova, E., Comparison of Interfacial Electron Transfer Efficiency in [Fe(ctpy)₂]²⁺-TiO₂ and [Fe(cCNC)₂]²⁺-TiO₂ Assemblies: Importance of Conformational Sampling. *J. Phys. Chem. A* **2018**, 122 (7), 1821-1830.
8. Liu, C.; Jakubikova, E., Two-step model for ultrafast interfacial electron transfer: limitations of Fermi's golden rule revealed by quantum dynamics simulations. *Chem. Sci.* **2017**, 8 (9), 5979-5991.
9. Jamula, L. L.; Brown, A. M.; Guo, D.; McCusker, J. K., Synthesis and characterization of a high-symmetry ferrous polypyridyl complex: approaching the ⁵T₂/³T₁ crossing point for Fe(II). *Inorg. Chem.* **2014**, 53 (1), 15-17.
10. Estrada-Montaña, A. S.; Ryabov, A. D.; Gries, A.; Gaiddon, C.; Le Lagadec, R., Iron(III) Pincer Complexes as a Strategy for Anticancer Studies. *Eur. J. Inorg. Chem.* **2017**, 2017 (12), 1673-1678.
11. Breivogel, A.; Wooh, S.; Dietrich, J.; Kim, T. Y.; Kang, Y. S.; Char, K.; Heinze, K., Anchor-Functionalized Push-Pull-Substituted Bis(tridentate) Ruthenium(II) Polypyridine Chromophores: Photostability and Evaluation as Photosensitizers. *Eur. J. Inorg. Chem.* **2014**, 2014 (16), 2720-2734.
12. Jakubikova, E.; Bowman, D. N., Fe(II)-Polypyridines as Chromophores in Dye-Sensitized Solar Cells: A Computational Perspective. *Acc. Chem. Res.* **2015**, 48 (5), 1441-1449.
13. Mukherjee, S.; Bowman, D. N.; Jakubikova, E., Cyclometalated Fe(II) Complexes as Sensitizers in Dye-Sensitized Solar Cells. *Inorg. Chem.* **2015**, 54 (2), 560-569.
14. Rego, L. G. C.; Batista, V. S., Quantum dynamics simulations of interfacial electron transfer in sensitized TiO₂ semiconductors. *J. Am. Chem. Soc.* **2003**, 125 (26), 7989-7997.